

RESEARCH

Open Access



Isolation and molecular characterization of the *Salmonella* Typhimurium orphan phage Arash

Mohammad Hashem Yousefi¹, Jeroen Wagemans², Seyed Shahram Shekarforoush¹, Marta Vallino³, Nadiia Pozhydaieva⁴, Katharina Höfer⁴, Rob Lavigne² and Saeid Hosseinzadeh^{1*}

Abstract

The current threat of multidrug resistant strains necessitates development of alternatives to antibiotics such as bacteriophages. This study describes the isolation and characterization of a novel *Salmonella* Typhimurium phage 'Arash' from hospital wastewater in Leuven, Belgium. Arash has a myovirus morphology with a 95 nm capsid and a 140 nm tail. The host range of Arash is restricted to its isolation host. Approximately 86% of the phage particles are adsorbed to a host cell within 10 min. Arash has latent period of 65 min and burst size of 425 PFU/cell. Arash has a dsDNA genome of 180,819 bp with GC content of 53.02% with no similarities to any characterized phages, suggesting Arash as a novel species in the novel 'Arashvirus' genus. Arash carries no apparent lysogeny-, antibiotic resistance- nor virulence-related genes. Proteome analysis revealed 116 proteins as part of the mature phage particles of which 27 could be assigned a function. Therefore, the present findings shed light on the morphological, microbiological and genomic characteristics of Arash and suggest its potential application as therapeutic and/or biocontrol agent.

Keywords Bacteriophage, *Salmonella* Typhimurium, Novel phage genus, 'Arashvirus'

Introduction

Non-typhoidal *Salmonella* spp. (NTS) are considered as one of the most serious zoonotic foodborne pathogens causing 155,000 deaths from diarrhea annually worldwide [1, 2]. It is the most frequently isolated pathogens in foodborne outbreaks in the European Union, with more than 91,000 salmonellosis cases each year [3, 4].

In Belgium alone, approximately 3,000 people become infected annually [5]. The symptoms of salmonellosis include fever, nausea, vomiting, abdominal cramps and inflammatory diarrhea. Furthermore, salmonellosis can lead to bacteremia and septicemia, followed by hospitalization and even death in severe cases, particularly in immunodeficient persons [6]. Around 50% of NTS infections are estimated to originate from contaminated food products [7, 8] with fresh-cut products, raw and undercooked meat, poultry and eggs being highly reported food commodities with *Salmonella* contamination [9, 10].

Among the NTS serovars, *S. Typhimurium* and *S. Enteritidis* are the most important serovars that cause self-limiting enterocolitis in humans [11]. Especially *S. Typhimurium* is more critical because of its broad host

*Correspondence:

Saeid Hosseinzadeh
hosseinzadeh@shirazu.ac.ir

¹Department of Food Hygiene and Public Health, School of Veterinary Medicine, Shiraz University, Shiraz 71946-84471, Iran

²Department of Biosystems, KU Leuven, Leuven 3001, Belgium

³Institute of Sustainable Plant Protection, National Research Council of Italy, Turin 10135, Italy

⁴Max Planck Institute for Terrestrial Microbiology, SYNMIKRO, Karl-von-Frisch-Strasse 16, Marburg 35043, Germany



© The Author(s) 2023. **Open Access** This article is licensed under a Creative Commons Attribution 4.0 International License, which permits use, sharing, adaptation, distribution and reproduction in any medium or format, as long as you give appropriate credit to the original author(s) and the source, provide a link to the Creative Commons licence, and indicate if changes were made. The images or other third party material in this article are included in the article's Creative Commons licence, unless indicated otherwise in a credit line to the material. If material is not included in the article's Creative Commons licence and your intended use is not permitted by statutory regulation or exceeds the permitted use, you will need to obtain permission directly from the copyright holder. To view a copy of this licence, visit <http://creativecommons.org/licenses/by/4.0/>. The Creative Commons Public Domain Dedication waiver (<http://creativecommons.org/publicdomain/zero/1.0/>) applies to the data made available in this article, unless otherwise stated in a credit line to the data.

range and zoonotic potential [12]. Moreover, multidrug resistant (MDR) *Salmonella* strains of both serovars have been isolated from humans, animals and the human food chain [13, 14]. MDR *Salmonella* strains are resistant to clinically relevant antibiotics including third-generation cephalosporins and fluoroquinolones [15, 16]. The emergence of these MDR strains results in economic losses in food production industries and complicates their containment [17–19]. In addition, MDR strains are responsible for the majority of *S. Typhimurium* outbreaks [20]. Inappropriate use of antibiotics in poultry and other farm animals is one of the reasons for the urging problem with MDR *Salmonella* strains in clinical samples [21].

Phages are types of viruses that specifically infect bacterial cells as their host and replicate only in them and are almost 50 times smaller than their host cells [22]. They are ubiquitous in environmental sources including human and animal feces, sewage and food [23]. Today, bacteriophages are receiving attention as antibacterials to deal with antibiotic-resistant pathogens in medicine, veterinary medicine, and food and agriculture industries. This is explained by their high specificity (up to the strain level), self-replication and rapid antimicrobial action. They are also low-cost to produce and can readily be isolated from all natural environments [24]. Phages do not harm eukaryotic cells and have received a “Generally Recognized As Safe” status. They also received halal and kosher certifications [25–28]. Some commercial phage products like SalmoFresh, Armament and Salmo-nex have been marketed for biocontrol of *Salmonella* spp. in food products [24, 29]. Moreover, phages have played a very key role in understanding the fundamental principles of molecular biology. The identification of CRISPR-Cas anti-phage defense systems followed by the development of the concept of gene editing has led to enormous developments in biology [30, 31]. Phages also can be employed in advanced biotechnological applications including bacterial detection, drug delivery vehicles, vaccine development and designing cheap and stable sensors for diagnostic assays [32].

In the present study, we isolated and characterized a novel *S. Typhimurium* bacteriophage from hospital and municipal sewage from Belgium. Based on whole genome sequencing, phage Arash represents a new genus with therapeutic or biocontrol potential in further applications.

Materials and methods

Phage isolation, purification, and propagation

Phage isolation was based on the method previously presented by Wang et al. (2017) with slight modifications [33]. Several hospital and municipal sewage samples were collected aseptically and kept at 4 °C for 24 h to allow settling of the debris and bigger particles. Next, 10 ml of

each sample were centrifuged at 6,000 ×g for 10 min at 4 °C, followed by filtration of the supernatant through 0.22 µm syringe filters. 100 µl of each filtrate and 300 µl of an overnight culture of *S. Typhimurium* ATCC 14,028 were added to 50 ml of Lysogeny broth (LB) medium and incubated for 24 h at 37 °C with agitation (160 rpm). After incubation, the suspension was centrifuged for 10 min at 4 °C and 6,000 ×g and filtered again. The filtrate was then serially diluted in phage buffer (10 mM Tris.HCl, 150 mM NaCl, 10 mM MgSO₄; pH 7.5). Subsequently, 100 µl of each dilution was mixed with 300 µl of an overnight bacterial suspension in 4 ml of soft agar (LB broth with 0.7% [w/v] agar) and poured onto solid LB agar plates (1.5% [w/v] agar) (double layer agar (DLA) method). Once the top layer was completely set, plates were incubated overnight for 18 h at 37 °C. Observation of transparent plaques indicated lack of bacterial growth. A single plaque was picked and suspended in 3 ml phage buffer, diluted and re-cultured using the DLA method. To ensure purity of the phage, this stage was repeated three times.

To propagate the isolated phage for further use and storage first, 10 ml of a fresh bacterial suspension with an OD at 600 nm (OD₆₀₀) of 0.6 (approximately 10⁸ CFU/ml) was added to 100 ml of LB supplemented with 10 mM MgSO₄, and the mixture was incubated at 37 °C. After 1 h, 100 µl of phage suspension was added and the incubation continued at 37 °C and 160 rpm for 24 h. Then, the mixture was centrifuged at 6,000 ×g for 10 min, the supernatant was filtered, and the phage titer was counted for further uses.

Morphology analysis by Transmission Electron Microscopy

The method presented by Vallino et al. (2021) was used for taking transmission electron micrographs (TEM) [34]. Briefly, 10 µl of the pure phage stock was deposited on carbon and formvar-coated 400 mesh grids (Gilder, Grantham Lincolnshire, England) and negatively stained with aqueous 0.5% w/v uranyl acetate. Observations and photographs were made using a Philips CM 10 transmission electron microscope (Eindhoven, The Netherlands), operating at 60 kV.

Phage titration and host range testing

To determine the phage titer and bacterial susceptibility, 100 µl of an overnight bacterial culture was plated using the DLA method. Once the top layer was solidified, diluted phage suspensions were dropped on the top layer in equal amounts of 10 µl. The plates were incubated at 37 °C for 24 h. For the host range assay, several Gram-negative bacterial strains, including *Salmonella* spp., *Hafnia alvei*, *Morganella morganii*, *Citrobacter* spp., *Escherichia coli* and *Klebsiella* spp. were tested for phage susceptibility (Table 1). This was performed in

triplicate. The *Salmonella* strains were serotyped using whole genome sequencing (Illumina MiniSeq, 2*150 bp, Nextera Flex library kit), followed by a SeqSero2 v1.1.0 analysis [35].

Phage adsorption assay

Bacteriophage adsorption was determined by enumeration of non-adsorbed phage to the host (*S. Typhimurium* ATCC 14,028) bacteria (free phage). For this purpose, the method described by Denes et al., 2015 was applied, with some modifications [36]. First, a phage suspension at 10^7 PFU/ml and a fresh exponential bacterial culture (OD_{600} of 0.6) was prepared. One hundred μ l of the phage suspension was added to 1 ml of the bacterial culture to have a multiplicity of infection (MOI) of 0.01. The infected cultures were agitated. Next, 5, 10 and 15 min after the start of infection, 100 μ l aliquots were taken, quickly diluted with 900 μ l of phage buffer and passed through a 0.22 μ m filter to obtain the free phage. Finally, the free phage count was determined in triplicate. The phage count at time 0 was measured by adding the phage suspension to a sterile culture (without host). The adsorption curve was measured three times.

One-step growth curve

The one-step growth curve of the phage was determined as described by Duc et al. (2018), with some modifications [37]. The phage suspension (MOI of 0.01) was mixed with 10 ml of *S. Typhimurium* ATCC 14,028 culture (OD_{600} of 0.3 equivalent to 10^8 CFU/ml). The mixture was incubated for 15 min at 37 °C to allow adsorption. Subsequently, the suspension was diluted (10^{-3} , 10^{-4} , 10^{-5} , 10^{-6}) and incubated at 37 °C for 180 min. An aliquot was taken every 5 to 10 min and titered. The experiment was performed in three replicates. The burst size was determined by dividing the number of phages formed during the rise period with the estimated number of infected cells at the latent period time [38].

Killing curve

Killing curves were performed according to James et al. (2020) [39]. Fresh bacterial culture (*S. Typhimurium* ATCC 14,028) at an OD_{600} of 0.6 ($\sim 10^8$ CFU/ml) (total volume of 200 μ l in a 96-well microplate) was infected with different concentrations of phage to obtain final MOIs of 0.1, 1, 10 and 100. Positive and negative controls were also considered by excluding the phage or bacterial cells, respectively. Finally, the plate was incubated at 37 °C in a microplate reader (CLARIO star Plus, BMG Labtech, Ortenberg, Germany) for 13 h. The OD_{600} of each well was measured at 30 min intervals. The experiment was performed in three replicates.

Whole genome sequencing & proteome analysis

Phage DNA isolation, whole genome sequencing, and annotation was performed as described in Azari et al. (2023) [40]. Briefly, Sequencing was carried out on an Illumina (San Diego, CA, USA) MiniSeq device. The raw sequencing data were assembled using SPAdes [41] and then the most related phages were identified using BLASTn [42] and Viptree v1.9 [43]. To investigate phage taxonomy, intergenomic similarities was calculated using VIRIDIC [44] and vConTACT2 [45]. Genome annotation was executed with RASTtk [46], BLASTp and HHPred [47]. A genome was created with Easyfig [48].

A phage suspension with a concentration of approximately 10^{10} PFU/ml was used to determine the phage's structural proteome. First, Arash was purified using a sucrose gradient ranging from 0 to 45%. The gradient was created in TM buffer (50 mM Tris-HCl, 10 mM $MgCl_2$, pH 7.5). 500 μ L of the phage solution was layered onto the top of the gradient. Subsequently, centrifugation was performed at 70,000 x g, 20 min, 4 °C. The resulting gradient fraction, containing the phages, was collected using a blunt cannula and then transferred to a new ultracentrifugation tube. To the collected fraction, 30 mL of ice-cold TM buffer were added. The phage particles were then pelleted through centrifugation at 100,000 x g, 1 h, 4 °C. After discarding the supernatant, the pellet was resuspended in 500 μ L of TM buffer and incubated at 4 °C overnight. The isolated phages were subjected to lysis buffer (50 mM Tris-HCl, pH 7.5, 1% SLS, 2 mM TCEP) and heated to 95 °C, 10 min. A sonication step (10 s, 20% amplitude, 0.5 pulse) was performed to degrade nucleic acids in the samples. Following this, iodoacetamide was added to the final concentration of 4 mM, and the samples were incubated for 30 min under light protection. The proteins were precipitated using acetone. The resulting pellets were washed with 500 μ L of methanol (-80 °C), air-dried, and resuspended in 50 μ L of resuspension buffer (50 mM Tris-HCl, pH 7.5, 0.5% SLS). The protein concentration was determined using the BCA assay (Pierce TM, BCA protein assay kit, ThermoFisher Scientific, Waltham, MA, USA). To 10 μ g of isolated proteins, 0.5 μ g of sequencing-grade trypsin (Promega) was added. Digestion was carried out overnight at 30 °C. The remaining SLS was precipitated by adding 1.5% TFA (v/v) and subsequent centrifugation at 4 °C, 17,000 x g, 10 min. The resulting supernatant was desalted for mass spectrometric analysis using C18 solid-phase columns (Chromabond C18 spin columns, Macherey Nagel, Düren, Germany) and then analyzed using liquid-chromatography-mass spectrometry (LC-MS) carried out on an Exploris 480 instrument connected to an Ultimate 3000 RSLC nano and a nanospray flex ion source (all Thermo Scientific). Peptide separation was performed on a reverse phase HPLC column (75 μ m x 42 cm) packed

in-house with C18 resin (2.4 μm ; Dr. Maisch). The following separating gradient was used: 98% solvent A (0.15% formic acid) and 5% solvent B (99.85% acetonitrile, 0.15% formic acid) to 30% solvent B over 45 min at a flow rate of 300 nl/min.

The data acquisition mode was set to obtain one high resolution MS scan at a resolution of 60,000 full width at half maximum (at m/z 200) followed by MS/MS scans of the most intense ions within 1 s (cycle 1s). To increase the efficiency of MS/MS attempts, the charged state screening modus was enabled to exclude unassigned and singly charged ions. The dynamic exclusion duration was set to 14 s. The ion accumulation time was set to 50 ms (MS) and 50 ms at 17,500 resolution (MS/MS). The automatic gain control (AGC) was set to 3×10^6 for MS survey scan and 2×10^5 for MS/MS scans.

For spectral based assessment MS raw files searches were carried out using MSFragger embedded within Scaffold 4 (Proteome Software) with 20 ppm peptide and fragment tolerance with Carbamidomethylation (C) as fixed, and oxidation (M) as variable modification using a customized phage protein database (based on the phage genome annotation).

NCBI accession number

The genome information is available on NCBI GenBank under accession number OQ632216.

Table 1 Host range analysis of phage Arash

Species	Strain	Source	Lysis*
<i>Salmonella</i> Typhimurium	ATCC 14,028	Reference strain	+
<i>Salmonella</i> Typhimurium	LT2	Reference strain	-
<i>Salmonella</i> Enteritidis	ATCC 13,076	Reference strain	LFW
<i>Salmonella</i> Enteritidis	ATCC 13,046	Reference strain	LFW
<i>Salmonella</i> Enteritidis	S42	Retail chicken	LFW
<i>Salmonella</i> Enteritidis	S2	Retail chicken	-
<i>Klebsiella pneumoniae</i>	2	Human infection	-
<i>Klebsiella</i> spp.	K1b	Wild-unknown source	-
<i>Hafnia alvei</i>	S44	Retail chicken	LFW
<i>H. alvei</i>	S31	Retail chicken	-
<i>H. alvei</i>	S439	Retail chicken	LFW
<i>Citrobacter</i> spp.	S53	Retail chicken	-
<i>Morganella morganii</i>	S257	Retail chicken	-
<i>M. morganii</i>	S28.1	Retail chicken	-
<i>E. coli</i>	MG1655	K12 reference strain	-
<i>E. coli</i>	E95	Milk	LFW
<i>E. coli</i>	E94	Milk	-
<i>E. coli</i>	E96	Milk	-
<i>E. coli</i>	E105	Milk	-

*Productive infection: +; Lysis from without: LFW; no lysis: -

Results and discussion

Among raw samples from various sources, four phages were isolated: two from hospital sewage, one from municipal sewage and the last one from a pig farm. Since three phages were very similar to previously described *Chivirus* phages, this study will focus on one novel phage isolated from hospital sewage (University Hospitals Leuven), which was called Arash. The naming of this phage was inspired by the Persian mythology heroic figure, Arash the Archer (Āraš-e Kamāngir).

Arash is a myovirus with a narrow host range

TEM revealed that Arash is a myovirus with an icosahedral head (95.80 ± 2.04 nm in diameter) and a contractile tail (140.47 ± 1.05 nm in length) (Fig. 1A). Its host range data is presented in Table 1. Arash forms a lysis zone for seven bacterial strains out of 19 tested strains, including a reference strain (the isolation host), several *Salmonella* Enteritidis strains, two *H. alvei* strains isolated from retail chicken and one *E. coli* strain isolated from milk. However, it only produces plaques on its isolation host strain *Salmonella* Typhimurium ATCC 14,028 (Supplementary Figure S1) and therefore can be considered a narrow host range spectrum based on the available collection of strains.

Microbiological characterization of Arash

Arash adsorbs relatively efficiently, with more than 86% of the phages being bound in the first 10 min followed by a gradual increase to 98.8% in the next 5 min (Fig. 1B). As explained by Abedon (2011), one key factor in measuring the antibacterial effect of a phage is phage adsorption. Therefore, phages like Arash which have a relatively fast adsorption rate are more likely to be beneficial for biocontrol or therapy purposes [49]. A one-step growth curve (Fig. 1C) indicates that Arash has a latent period of 65 min, with a relatively high burst size of 425 PFU/cell, also beneficial for future applications. Next, killing curves were made. As illustrated in Fig. 2, the higher the MOI, the faster the bactericidal activity is observed. At an MOI of 100, regrowth of a resistant population is observed around 3 to 4 h after infection. At an MOI of 10, the population seems to be controlled for the longest period. According to Islam et al. (2020a), phage LPST153 at MOIs of 0.1, 1, 10 and 100 was able to inhibit the growth of *S. Typhimurium* ATCC 13,311 in 12 h [50]. In another study by Islam et al. (2020b), the growth of *S. Typhimurium* UK-1 was efficiently inhibited by LPST94 at MOI 1 over 12 h. This phage also inhibited the growth of *S. Typhimurium* UK-1, *S. Typhimurium* ATCC 14,028, *S. Enteritidis* ATCC 13,076 and *S. Enteritidis* SGSC 4901 for 11–12 h at MOIs of 0.1, 1, 10 and 100 [51]. According to Esmael et al. (2021), the growth of *S. Typhimurium* EG.SmT3 was inhibited by the phages SPHG1 and

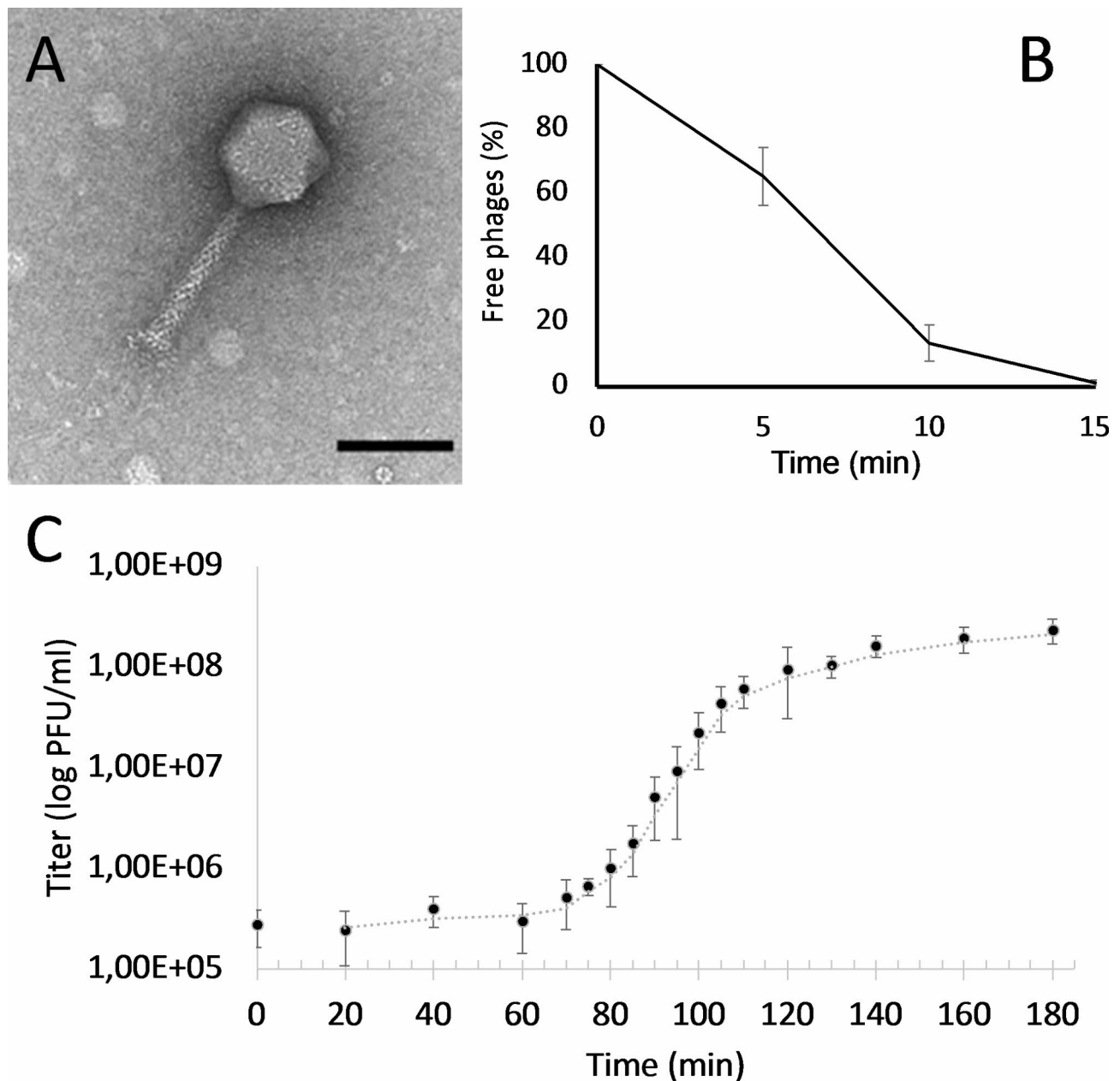


Fig. 1 Microbiological characterization of phage Arash. **(A)** Electron micrograph: TEM analysis shows a myovirus morphology for Arash (scale bar represents 100 nm). **(B)** Adsorption curve of Arash: more than 86% of the phages are being bound in the first 10 min followed by a gradual increase to 98.8% in the next 5 min. **(C)** One-step growth curve: Arash has a latent period of 65 min, with a high burst size of 425 PFU/cell

SPHG3 for 6 h at 0.1, 1, and 5. However, the application of MOI 0.01 did not successfully inhibit the growth of bacteria as much as the other MOIs, especially after 2 h [52].

Arash is a novel phage from a yet unclassified genus

Whole genome analysis revealed that phage Arash has a dsDNA genome of 180,819 bp with a GC content of 53.02%. Both BLASTn and Viptree showed no significant similarities to any previously characterized phages. Therefore, phage Arash can be considered a novel species

in the novel 'Arashvirus' genus within a yet unclassified family (Supplementary Figure S2). This was confirmed using a vConTACT2 gene-sharing network analysis, identifying Arash as a singleton when compared to the NCBI viral RefSeq database. Next, a neighbour joining-tree (1,000 bootstraps) was constructed for the terminase protein, the major capsid protein and the DNA polymerase to compare these Arash proteins to the corresponding proteins of phages identified by VipTree as having a similar proteome (Fig. 3). Only the terminase of Arash clusters consistently (in 90% of the bootstraps)

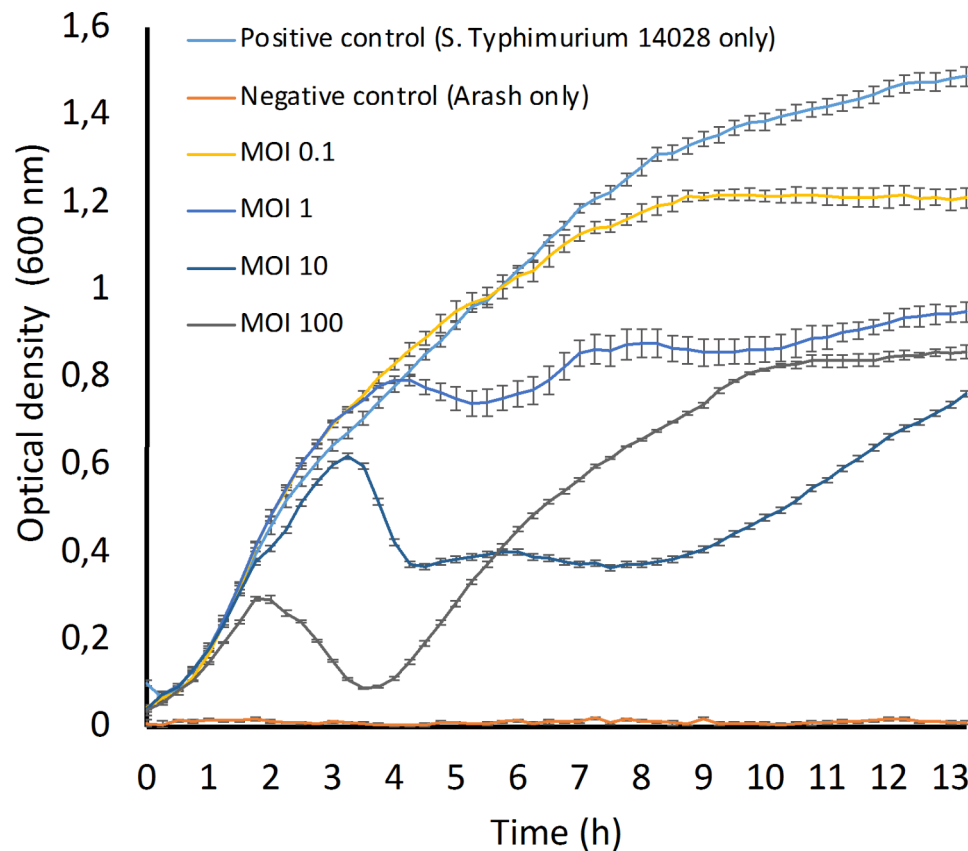


Fig. 2 Killing curve of phage Arash in different MOIs. *S. Typhimurium* 14,028 was infected with Arash at different MOIs. The optical density was followed over time. Each point represents the average of three replicates and its standard deviation. As positive control, a culture without phage was monitored. As negative control, a phage only sample was measured over time

together with a known terminase of *Colwellia* phage 9A (NC_018088.1). However, on the nucleotide level, there is no similarity at all between Arash and 9A.

Based on the structural annotation, 252 coding sequences and 21 tRNAs were identified (Supplementary Table S1). Only 50 coding sequences encode proteins that could be assigned a putative function (19.8%), while the remaining CDSs (80.2%) encode hypothetical proteins (Fig. 4). Within the functionally annotated genes, no lysogenic lifecycle, antibiotic resistance- nor virulence-related genes could be retrieved, suggesting Arash can be safely used for biocontrol or therapy applications from a genomics perspective.

Since the vast majority of the genes remained unknown and a novel genus is proposed, a tandem mass spectrometry structural proteome analysis was performed (Table 2). Proteins with less than two unique identified peptides were considered as false positives and were not reported. Based on these criteria, 116 proteins could positively be identified as part of the mature phage particles. Of these, 27 were previously assigned a function based on similarity to known proteins. Eighty-eight were re-annotated as structural proteins, reducing the total percentage

of ‘dark matter’ (i.e. unknown ORFs) in the genome from 80.2 to 48.0%.

The DNA-directed RNA polymerase (subunit beta) Gp206 is the protein detected the most, with 3516 total spectrum counts, followed by the structural proteins Gp4 and Gp229, the major capsid protein Gp226 and the beta’ subunit of the RNA polymerase Gp216 with respectively, 1952, 1345, 1333 and 1210 counts. Besides this beta and beta’ subunits, several enzymes are detected in the virus particles such as the cell wall hydrolase (Gp8), the RNA polymerase subunits sigma (Gp10), two ribonucleotide reductases (Gp27 and Gp61), two RNA ligases (Gp120 and Gp143) and a DNA helicase (Gp217) (Table 2). These enzymes might be directly needed at the start of infection such as the cell wall hydrolase for making a hole in the cell wall before injecting the phage DNA inside the host or e.g., the RNA polymerase for early transcription. Another possibility might be that these enzymes are expressed in large amounts during phage infection and are therefore still being present in the purified mature phage particles.

Generally phage Arash can be placed next to phages with a large genome or salmonella jumbo phages such as SPN3US, the collection of phages SPFM1 to SPFM22

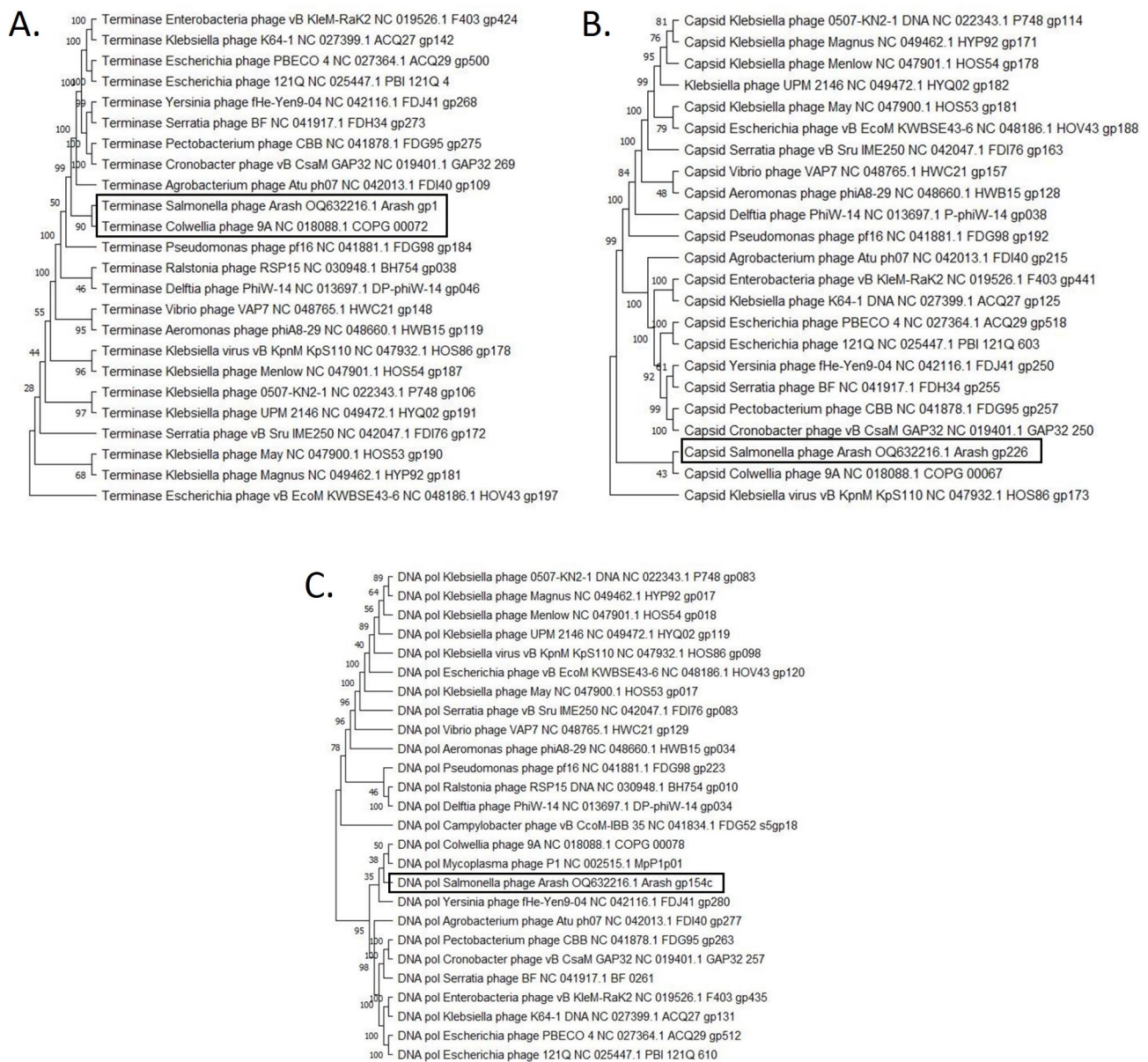


Fig. 3 Phylogenetic trees of Arash terminase (large subunit) (A), major capsid protein (B) and DNA polymerase (C). The consensus trees were constructed using the corresponding protein of Arash and related phages with MEGA X [53]. The amino acid sequences were aligned using MUSCLE and a neighbour-joining tree with 1,000 bootstraps was constructed

Arash, 181 kb

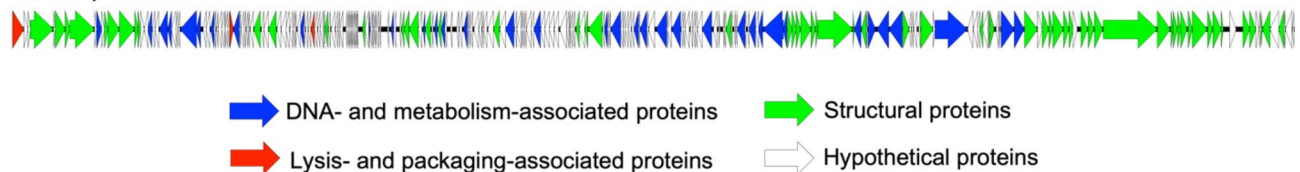


Fig. 4 Genome map of Arash. Each arrow represents a coding sequence. In red, genes encoding packaging and lysis-associated proteins are displayed, in green structural proteins and in blue DNA- and metabolism-associated proteins (adapted from EasyFig)

Table 2 Structural proteome of phage Arash. For each identified protein, the sequence coverage, the unique peptide count and the number of total detected spectra are reported. For proteins previously annotated as hypothetical, but now re-annotated as being structural, the functional annotation is italicized

Protein	Functional annotation	Coverage	# Unique Peptides	# Spectra
Gp004	<i>Structural protein</i>	87,88%	60	1952
Gp006	<i>Structural protein</i>	87,66%	16	280
Gp007	<i>Structural protein</i>	76,99%	7	202
Gp008	Cell wall hydrolase, structural protein	80,52%	44	777
Gp010	RNA polymerase sigma factor RpoS	100,00%	24	467
Gp011	<i>Structural protein</i>	100,00%	2	156
Gp012	<i>Structural protein</i>	77,38%	7	253
Gp013	<i>Structural protein</i>	82,95%	29	517
Gp014	<i>Structural protein</i>	60,44%	15	474
Gp015	<i>Structural protein</i>	76,22%	4	160
Gp016	<i>Structural protein</i>	100,00%	10	222
Gp017	<i>Structural protein</i>	64,67%	3	80
Gp019	Deoxynucleoside monophosphate kinase	100,00%	5	116
Gp021	<i>Structural protein</i>	89,13%	2	324
Gp023	Pyrophosphatase	53,14%	3	173
Gp024	<i>Structural protein</i>	97,60%	10	273
Gp026	<i>Structural protein</i>	100,00%	2	31
Gp027	Ribonucleotide reductase of class Ia (aerobic), alpha subunit	93,06%	11	663
Gp028	Phosphohydrolase	56,85%	2	56
Gp029	<i>Structural protein</i>	98,04%	3	90
Gp040	Pyrophosphohydrolase	99,64%	3	253
Gp042	<i>Structural protein</i>	73,38%	3	150
Gp046	<i>Structural protein</i>	100,00%	4	67
Gp047	<i>Structural protein</i>	89,03%	7	331
Gp049	<i>Structural protein</i>	100,00%	8	307
Gp050	<i>Structural protein</i>	73,08%	3	292
Gp051	<i>Structural protein</i>	100,00%	5	168
Gp052	<i>Structural protein</i>	99,16%	2	318
Gp057	<i>Structural protein</i>	100,00%	2	287
Gp058	Phosphoesterase	98,86%	3	76
Gp061	Ribonucleotide reductase of class Ia (aerobic), alpha subunit	100,00%	2	112
Gp065	<i>Structural protein</i>	76,28%	4	75
Gp067	<i>Structural protein</i>	77,48%	5	432
Gp070	<i>Structural protein</i>	100,00%	3	110
Gp071	<i>Structural protein</i>	95,40%	2	96
Gp082	<i>Structural protein</i>	87,50%	3	103
Gp089	<i>Structural protein</i>	100,00%	4	80
Gp092	HNH homing endonuclease	98,20%	2	193
Gp093	<i>Structural protein</i>	100,00%	3	115
Gp095	<i>Structural protein</i>	99,22%	5	406
Gp096	<i>Structural protein</i>	98,22%	15	816
Gp097	<i>Structural protein</i>	97,27%	24	1060
Gp100	<i>Structural protein</i>	98,84%	9	471
Gp103	<i>Structural protein</i>	100,00%	10	164
Gp113	<i>Structural protein</i>	90,58%	4	160
Gp117	<i>Structural protein</i>	84,29%	2	305
Gp118	<i>Structural protein</i>	88,76%	9	265
Gp120	RNA ligase	70,63%	3	300
Gp121	<i>Structural protein</i>	100,00%	3	209

Table 2 (continued)

Protein	Functional annotation	Coverage	# Unique Peptides	# Spectra
Gp129	Structural protein	87,11%	4	246
Gp132	Structural protein	72,22%	6	121
Gp134	Structural protein	100,00%	2	91
Gp138	Structural protein	100,00%	9	180
Gp140	Structural protein	100,00%	13	334
Gp141	Structural protein	87,87%	26	836
Gp143	RNA ligase	100,00%	14	204
Gp149	Structural protein	100,00%	2	140
Gp151	Structural protein	100,00%	2	98
Gp156	Structural protein	100,00%	9	469
Gp157	Nicotinamide phosphoribosyltransferase	74,21%	3	423
Gp159	Structural protein	80,72%	5	195
Gp165	Structural protein	100,00%	2	254
Gp167	Structural protein	83,83%	2	179
Gp168	Uracil DNA glycosylase	98,66%	3	513
Gp169	Structural protein	55,03%	6	259
Gp173	Structural protein	100,00%	16	299
Gp177	DNA ligase	100,00%	2	495
Gp182	RNA exonuclease	90,24%	6	160
Gp183	DNA primase	89,74%	2	932
Gp185	Structural protein	100,00%	9	301
Gp186	Structural protein	100,00%	8	98
Gp187	Structural protein	100,00%	9	221
Gp188	Structural protein	100,00%	30	561
Gp190	Tail fiber protein	51,40%	4	92
Gp191	Tail protein	79,96%	58	832
Gp193	ATP-dependent DNA helicase	92,28%	2	217
Gp194	Structural protein	100,00%	9	159
Gp197	ATP-dependent DNA helicase	93,11%	2	517
Gp199	Structural protein	70,00%	9	245
Gp202	Structural protein	79,59%	6	125
Gp204	Portal protein	93,44%	32	877
Gp206	DNA-directed RNA polymerase subunit beta	100,00%	128	3516
Gp210	Structural protein	100,00%	7	111
Gp213	Structural protein	93,46%	7	143
Gp216	DNA-directed RNA polymerase subunit beta'	89,11%	40	1210
Gp217	DNA helicase	100,00%	38	1148
Gp218	Structural protein	89,11%	36	1149
Gp220	Structural protein	95,77%	6	289
Gp221	Structural protein	100,00%	8	355
Gp222	Structural protein	84,93%	16	365
Gp223	Structural protein	100,00%	9	283
Gp224	Structural protein	100,00%	8	222
Gp225	Structural protein	80,00%	2	203
Gp225.1	Structural protein	100,00%	14	582
Gp226	Major capsid protein	86,64%	30	1333
Gp227	Major tail protein	72,08%	17	406
Gp228	Structural protein	80,57%	12	117
Gp229	Structural protein	68,84%	79	1345
Gp230	Structural protein	60,49%	20	245
Gp231	Structural protein	97,09%	5	244
Gp232	Structural protein	100,00%	9	172

Table 2 (continued)

Protein	Functional annotation	Coverage	# Unique Peptides	# Spectra
Gp233	Structural protein	100,00%	7	137
Gp234	Structural protein	87,16%	11	397
Gp235	Structural protein	100,00%	10	258
Gp236	Structural protein	80,59%	32	689
Gp237	Structural protein	89,57%	11	356
Gp238	Structural protein	90,26%	12	371
Gp239	PAAR-repeat central spike tip protein	100,00%	2	126
Gp242	Structural protein	100,00%	21	550
Gp243	Structural protein	100,00%	12	359
Gp244	Structural protein	80,50%	3	80
Gp246	Structural protein	100,00%	5	95
Gp247	Structural protein	77,17%	3	430
Gp248	Structural protein	61,41%	2	369
Gp249	Structural protein	100,00%	5	226
Gp251	Structural protein	76,25%	2	379

and phage pSal-SNUABM-04. However Arash with an 180,819 bp genome is smaller than the mentioned phages. For instance, phage SPN3US, phages SPFM1 to SPFM22 and phage pSal-SNUABM possess genomes sizes of 240,413, 233,195 to 242,624 and 239,626 bp, respectively. On the other hand Arash has a GC content of 53.02% while this for the mentioned phages was 48.54, 48.57 to 48.88 and 51.56%, respectively [54–56].

Conclusion and perspectives

With the ever-increasing interest in the application of phages as antibacterial agents, the number of new phage genomes with little to no homology to any phages in the database will also keep on increasing. This creates unique opportunities to investigate the taxonomical similarity of bacteriophages based on their genome sequences. In this research, a novel phage from an unclassified, proposed genus ‘Arashvirus’ was isolated from the sewage of University Hospitals Leuven, Belgium and named phage Arash. Despite its narrow host range, Arash can be considered as a potential tool to deal with specific *S. Typhimurium* strains, both in the food industry and in human and animal infections, due to its many useful features, including its relatively fast adsorption, high burst size and the lack of antibiotic resistance, lysogenic and virulence factors in its genome.

Supplementary Information

The online version contains supplementary material available at <https://doi.org/10.1186/s12866-023-03056-9>.

Supplementary Material 1

Supplementary Material 2

Acknowledgements

The authors would like to express their sincere appreciation to the Shiraz University. Also we appreciate the staff of the Laboratory of Gene Technology (LoGT), KU Leuven, Leuven, Belgium (Alison Kerremans, Sayali Gorivale and Claudia Campobasso) and department of Food Hygiene and Quality Control, Shiraz University, Shiraz, Iran for their esteemed collaboration in this study. We also thank Dr. Timo Glatter of the Proteomics facility of the Max Planck Institute for his help with the MS.

Authors' contributions

Conceptualization by M.H.Y. and J.W. and S.H.; Methodology by M.H.Y., M.V., N.P. and K.H.; Software by M.H.Y. and J.W.; Analysis by M.H.Y. and J.W.; Draft Writing by M.H.Y. and J.W.; Review and Editing by S.H., J.W., S.S.S. and R.L.; Visualization by J.W. and M.V.; Supervision by S.H. and J.W.; Funding by S.H. and J.W.; All authors have read and agreed to the published version of the manuscript.

Funding

This study was supported by internal funding of Shiraz University.

Data Availability

The *S. Typhimurium* phage genome sequence was deposited in NCBI. The accession number is OQ632216.

Declarations

Ethics approval and consent to participate

Not applicable.

Consent for publication

None to declare.

Competing interests

None to declare.

Received: 5 June 2023 / Accepted: 11 October 2023

Published online: 19 October 2023

References

1. Ao TT, Feasey NA, Gordon MA, Keddy KH, Angulo FJ, Crump JA. Global burden of invasive nontyphoidal *Salmonella* Disease, 2010. *Emerg Infect Dis.* 2015;21(6):941. <https://doi.org/10.3201/eid2106.140999>.

2. Organization WH. WHO estimates of the global burden of foodborne Diseases: foodborne Disease burden epidemiology reference group 2007–2015. World Health Organization; 2015.
3. Authority EFS, Prevention ECfD. Control. The European Union summary report on trends and sources of zoonoses, zoonotic agents and food-borne outbreaks in 2011. EFSA J. 2013;11(4):3129.
4. Wuyts V, Mattheus W, De Laminne de Bex G, Wildemaue C, Roosens NH, Marchal K, et al. MLVA as a tool for public health surveillance of human *Salmonella* Typhimurium: prospective study in Belgium and evaluation of MLVA loci stability. PLoS ONE. 2013;8(12):e84055. <https://doi.org/10.1371/journal.pone.0084055>.
5. Sciencono. Sciencono & Salmonellosis.
6. Acheson D, Hohmann EL. Nontyphoidal salmonellosis. Clin Infect Dis. 2001;32(2):263–9. Epub 2001 Jan 15. <https://doi.org/10.1086/318457>.
7. Havelaar AH, Kirk MD, Torgerson PR, Gibb HJ, Hald T, Lake RJ, et al. World Health Organization global estimates and regional comparisons of the burden of foodborne Disease in 2010. PLoS Med. 2015;12(12):e1001923. <https://doi.org/10.1371/journal.pmed.1001923>.
8. Kirk MD, Pires SM, Black RE, Caipo M, Crump JA, Devleeschauwer B, et al. World Health Organization estimates of the global and regional Disease burden of 22 foodborne bacterial, protozoal, and viral Diseases, 2010: a data synthesis. PLoS Med. 2015;12(12):e1001921. <https://doi.org/10.1371/journal.pmed.1001921>.
9. Brown EW, Bell R, Zhang G, Timme R, Zheng J, Hammack TS, et al. *Salmonella* genomics in public health and food safety. EcoSal Plus. 2021;9(2):eESP-0008. <https://doi.org/10.1128/ecosalplus.ESP-0008-2020>.
10. Control CfD. Prevention. Preliminary FoodNet data on the incidence of Infection with pathogens transmitted commonly through food—10 states, 2009. MMWR Morbidity and Mortality Weekly Report. 2010;59(14):418–22.
11. Stanaway JD, Parisi A, Sarkar K, Blacker BF, Reiner RC, Hay SI, et al. The global burden of non-typhoidal *Salmonella* invasive Disease: a systematic analysis for the global burden of Disease Study 2017. Lancet Infect Dis. 2019;19(12):1312–24. [https://doi.org/10.1016/S1473-3099\(19\)30418-9](https://doi.org/10.1016/S1473-3099(19)30418-9).
12. Xiang Y, Li F, Dong N, Tian S, Zhang H, Du X, et al. Investigation of a Salmonellosis outbreak caused by multidrug resistant *Salmonella* Typhimurium in China. Front Microbiol. 2020;11:801. <https://doi.org/10.3389/fmicb.2020.00801>.
13. Campos J, Mourão J, Peixe L, Antunes P. Non-typhoidal *Salmonella* in the pig production chain: a comprehensive analysis of its impact on human health. Pathogens. 2019;8(1):19. <https://doi.org/10.3390/pathogens8010019>.
14. Iwamoto M, Reynolds J, Karp BE, Tate H, Fedorka-Cray PJ, Plumblee JR, et al. Ceftriaxone-resistant nontyphoidal *Salmonella* from humans, retail meats, and food animals in the United States, 1996–2013. Foodborne Pathog Dis. 2017;14(2):74–83. <https://doi.org/10.1089/fpd.2016.2180>.
15. Argimón S, Nagaraj G, Shamanna V, Sravani D, Vasanth AK, Prasanna A, et al. Circulation of third-generation cephalosporin resistant *Salmonella* Typhi in Mumbai, India. Clin Infect Dis. 2022;74(12):2234–7. <https://doi.org/10.1093/cid/ciab897>.
16. Rasheed F, Saeed M, Alikhan N-F, Baker D, Khurshid M, Ainsworth EV, et al. Emergence of resistance to fluoroquinolones and third-generation cephalosporins in *Salmonella* Typhi in Lahore, Pakistan. Microorganisms. 2020;8(9):1336. <https://doi.org/10.3390/microorganisms8091336>.
17. Angulo FJ, Johnson KR, Tauxe RV. Origins and consequences of antimicrobial-resistant nontyphoidal *Salmonella*: implications for the use of fluoroquinolones in food animals. Microb Drug Resist. 2000;6(1):77–83. <https://doi.org/10.1089/mdr.2000.6.77>.
18. Frenzen P, Buzby J, Roberts T. An updated estimate of the economic costs of human illness due to food borne *Salmonella* in the United States. 1999.
19. Kariuki S, Gordon MA, Feasey N, Parry CM. Antimicrobial resistance and management of invasive *Salmonella* Disease. Vaccine. 2015;33:C21–C9. <https://doi.org/10.1016/j.vaccine.2015.03.102>.
20. Folster JP, Grass JE, Bicknese A, Taylor J, Friedman CR, Whichard JM. Characterization of resistance genes and plasmids from outbreaks and illness clusters caused by *Salmonella* resistant to ceftriaxone in the United States, 2011–2012. Microb Drug Resist. 2017;23(2):188–93. <https://doi.org/10.1089/mdr.2016.0080>.
21. Medalla F, Gu W, Mahon BE, Judd M, Folster J, Griffin PM, et al. Estimated incidence of antimicrobial drug-resistant nontyphoidal *Salmonella* Infections, United States, 2004–2012. Emerg Infect Dis. 2017;23(1):29. <https://doi.org/10.3201/eid2301.160771>.
22. Ly-Chatain MH. The factors affecting effectiveness of treatment in phages therapy. Front Microbiol. 2014;5:51. <https://doi.org/10.3389/fmicb.2014.00051>.
23. Gwak KM, Choi IY, Lee J, Oh J-H, Park M-K. Isolation and characterization of a lytic and highly specific phage against *Yersinia enterocolitica* as a novel biocontrol agent. J Microbiol Biotechnol. 2018. <https://doi.org/10.4014/jmb.1808.08001>.
24. Goodridge LD, Bisha B. Phage-based biocontrol strategies to reduce foodborne pathogens in foods. Bacteriophage. 2011;1(3):130–7. <https://doi.org/10.4161/bact.1.3.17629>.
25. Garcia P, Martinez B, Obeso J, Rodriguez A. Bacteriophages and their application in food safety. Lett Appl Microbiol. 2008;47(6):479–85. <https://doi.org/10.1111/j.1472-765X.2008.02458.x>.
26. Hagens S, Loessner MJ. Bacteriophage for biocontrol of foodborne pathogens: calculations and considerations. Curr Pharm Biotechnol. 2010;11(1):58–68. <https://doi.org/10.2174/138920110790725429>.
27. McCallin S, Sarker SA, Barretto C, Sultana S, Berger B, Huq S, et al. Safety analysis of a Russian phage cocktail: from metagenomic analysis to oral application in healthy human subjects. Virol. 2013;443(2):187–96. <https://doi.org/10.1016/j.virol.2013.05.022>.
28. Sarker SA, McCallin S, Barretto C, Berger B, Pittet A-C, Sultana S, et al. Oral T4-like phage cocktail application to healthy adult volunteers from Bangladesh. Virol. 2012;434(2):222–32. <https://doi.org/10.1016/j.virol.2012.09.002>.
29. Sukumaran AT, Nannapaneni R, Kiess A, Sharma CS. Reduction of *Salmonella* on chicken meat and chicken skin by combined or sequential application of lytic bacteriophage with chemical antimicrobials. Int J Food Microbiol. 2015;207:8–15. <https://doi.org/10.1016/j.ijfoodmicro.2015.04.025>.
30. Ansaldi M, Boulanger P, Brives C, Debarbieux L, Dufour N, Froissart R, et al. A century of research on bacteriophages. Virologie (Montrouge France). 2020;24(1):9–22. <https://doi.org/10.1684/vir.2020.0809>.
31. Westra ER, Van Houte S, Gandon S, Whitaker R. The ecology and evolution of microbial CRISPR-Cas adaptive immune systems. Philos Trans R Soc Lond B Biol Sci. 2019: 20190101. <https://doi.org/10.1098/rstb.2019.0101>.
32. Abril AG, Carrera M, Notario V, Sánchez-Pérez Á, Villa TG. The use of bacteriophages in biotechnology and recent insights into proteomics. Antibiotics. 2022;11(5):653. <https://doi.org/10.3390/antibiotics11050653>.
33. Wang C, Chen Q, Zhang C, Yang J, Lu Z, Lu F, et al. Characterization of a broad host-spectrum virulent *Salmonella* bacteriophage fmb-p1 and its application on duck meat. Virus Res. 2017;236:14–23. <https://doi.org/10.1016/j.virusres.2017.05.001>.
34. Vallino M, Rossi M, Ottati S, Martino G, Galetto L, Marzachi C, et al. Bacteriophage-host association in the phytoplasma insect vector *Euscelidius Variiegatus*. Pathogens. 2021;10(5):612. <https://doi.org/10.3390/pathogens10050612>.
35. Zhang S, den Bakker HC, Li S, Chen J, Dinsmore BA, Lane C, et al. SeqSero2: Rapid and Improved *Salmonella* Serotype determination using whole-genome sequencing data. Appl Environ Microbiol. 2019;85(23). <https://doi.org/10.1128/AEM.01746-19>.
36. Denes T, den Bakker HC, Tokman JI, Guldemann C, Wiedmann M. Selection and characterization of phage-resistant mutant strains of *Listeria monocytogenes* reveal host genes linked to phage adsorption. Appl Environ Microbiol. 2015;81(13):4295–305. <https://doi.org/10.1128/AEM.00087-15>.
37. Duc HM, Son HM, Honjoh K-i, Miyamoto T. Isolation and application of bacteriophages to reduce *Salmonella* contamination in raw chicken meat. LWT. 2018;91:353–60. <https://doi.org/10.1016/j.lwt.2018.01.072>.
38. Fanaei Pirlar R, Wagemans J, Kunisch F, Lavigne R, Trampuz A, Gonzalez Moreno M. Novel *Stenotrophomonas maltophilia* bacteriophage as potential therapeutic Agent. Pharmaceuticals. 2022;14(10):2216. <https://doi.org/10.3390/pharmaceutics14102216>.
39. James SL, Rabiye M, Neuman BW, Percival G, Jackson RW. Isolation, characterisation and experimental evolution of phage that infect the horse chestnut tree pathogen, *Pseudomonas syringae* Pv. *Aesculi*. Curr Microbiol. 2020;77:1438–47. <https://doi.org/10.1007/s00284-020-01952-1>.
40. Azari R, Yousefi MH, Taghipour Z, Wagemans J, Lavigne R, Hosseinzadeh S et al. Application of the lytic bacteriophage Rostam to control *Salmonella* Enteritidis in eggs. Int J Food Microbiol. 2023;110097. <https://doi.org/10.1016/j.ijfoodmicro.2023.110097>.
41. Bankevich A, Nurk S, Antipov D, Gurevich AA, Dvorkin M, Kulikov AS, et al. SPAdes: a new genome assembly algorithm and its applications to single-cell sequencing. J Comput Biol. 2012;19(5):455–77. <https://doi.org/10.1089/cmb.2012.0021>.

42. Altschul SF, Gish W, Miller W, Myers EW, Lipman DJ. Basic local alignment search tool. *J Mol Biol.* 1990;215(3):403–10. [https://doi.org/10.1016/S0022-2836\(05\)80360-2](https://doi.org/10.1016/S0022-2836(05)80360-2).
43. Nishimura Y, Yoshida T, Kuronishi M, Uehara H, Ogata H, Goto S. ViPTree: the viral proteomic tree server. *Bioinformatics.* 2017;33(15):2379–80. <https://doi.org/10.1093/bioinformatics/btx157>.
44. Moraru C, Varsani A, Kropinski AM. VIRIDIC—A novel tool to calculate the intergenomic similarities of prokaryote-infecting viruses. *Viruses.* 2020;12(11):1268. <https://doi.org/10.3390/v12111268>.
45. Bin Jang H, Bolduc B, Zablocki O, Kuhn JH, Roux S, Adriaenssens EM, et al. Taxonomic assignment of uncultivated prokaryotic virus genomes is enabled by gene-sharing networks. *Nat Biotechnol.* 2019;37(6):632–9. <https://doi.org/10.1038/s41587-019-0100-8>.
46. Brettin T, Davis JJ, Disz T, Edwards RA, Gerdes S, Olsen GJ, et al. RASTtk: a modular and extensible implementation of the RAST algorithm for building custom annotation pipelines and annotating batches of genomes. *Sci Rep.* 2015;5(1):8365. <https://doi.org/10.1038/srep08365>.
47. Soding J, Biegert A, Lupas AN. The HHpred interactive server for protein homology detection and structure prediction. *Nucleic Acids Res.* 2005;33(suppl2):W244–W8. <https://doi.org/10.1093/nar/gki408>.
48. Sullivan MJ, Petty NK, Beatson SA. Easyfig: a genome comparison visualizer. *Bioinformatics.* 2011;27(7):1009–10. <https://doi.org/10.1093/bioinformatics/btr039>.
49. Abedon ST. Lysis from without. *Bacteriophage.* 2011;1(1):46–9. <https://doi.org/10.4161/bact.1.1.13980>.
50. Islam MS, Hu Y, Mizan MFR, Yan T, Nime I, Zhou Y, et al. Characterization of *Salmonella* phage LPST153 that effectively targets most prevalent *Salmonella* serovars. *Microorganisms.* 2020;8(7):1089. <https://doi.org/10.3390/microorganisms8071089>.
51. Islam MS, Zhou Y, Liang L, Nime I, Yan T, Willias SP, et al. Application of a broad range lytic phage LPST94 for biological control of *Salmonella* in foods. *Microorganisms.* 2020;8(2):247. <https://doi.org/10.3390/microorganisms8020247>.
52. Esmael A, Azab E, Gobouri AA, Nasr-Eldin MA, Moustafa MM, Mohamed SA, et al. Isolation and characterization of two lytic bacteriophages infecting a multi-drug resistant *Salmonella* Typhimurium and their efficacy to combat Salmonellosis in ready-to-use foods. *Microorganisms.* 2021;9(2):423. <https://doi.org/10.3390/microorganisms9020423>.
53. Tamura K, Stecher G, Kumar S. MEGA11: Molecular Evolutionary Genetics Analysis Version 11. *Mol Biol Evol.* 2021;38(7):3022–7. <https://doi.org/10.1093/molbev/msab120>.
54. Kwon J, Kim SG, Kim HJ, Giri SS, Kim SW, Lee SB, et al. Isolation and characterization of *Salmonella* jumbo-phage pSal-SNUABM-04. *Viruses.* 2020;13(1):27. <https://doi.org/10.3390/v13010027>.
55. Lee J-H, Shin H, Kim H, Ryu S. Complete genome sequence of *Salmonella* bacteriophage SPN3US. *J Virol.* 2011. <https://doi.org/10.1128/JVI.06344-11>.
56. Thanki AM, Brown N, Millard AD, Clokie MR. Genomic characterization of jumbo *Salmonella* phages that effectively target United Kingdom pig-associated *Salmonella* serotypes. *Front Microbiol.* 2019;10:1491. <https://doi.org/10.3389/fmicb.2019.01491>.

Publisher's Note

Springer Nature remains neutral with regard to jurisdictional claims in published maps and institutional affiliations.